BJR

https://doi.org/10.1259/bjr.20170411

Received: 1 June 2017 | Revised: 5 September 2017 | Accepted: 13 September 2017

Cite this article as:
George E, Wortman JR, Fulwadhva UP, Uyeda JW, Sodickson AD. Dual energy CT applications in pancreatic pathologies. *Br J Radiol* 2017; **90**: 20170411.

REVIEW ARTICLE

Dual energy CT applications in pancreatic pathologies

ELIZABETH GEORGE, MD, JEREMY R WORTMAN, MD, URVI P FULWADHVA, MD, JENNIFER W UYEDA, MD and AARON D SODICKSON, MD, PhD

Department of Radiology, Division of Emergency Radiology, Brigham and Women's Hospital and Harvard Medical School, Boston, MA, USA

Address correspondence to: Dr Elizabeth George
E-mail: *egeorge6@partners.org*

ABSTRACT

Dual energy CT (DECT) is a technology that is gaining widespread acceptance, particularly for its abdominopelvic applications. Pancreatic pathologies are an ideal application for the many advantages offered by dual energy post-processing. This article reviews the current literature on dual energy CT pancreatic imaging, specifically in the evaluation of pancreatic adenocarcinoma, other solid and cystic pancreatic neoplasms, and pancreatitis. The advantages in characterization and quantification of enhancement, detection of subtle lesions, and potential reduction of imaging phases and contrast usage are reviewed. We also discuss directions for future research, and the ideal use of dual energy CT in routine clinical practice.

INTRODUCTION

The principle of dual energy CT (DECT), although envisioned in the 1970s, was not clinically applicable at that time due to technical limitations in scan time, slice thickness and the need for two separate acquisitions with the associated patient motion artefact and dose.[1–3] Advances in CT technology have overcome these limitations, making DECT a clinical reality. There is growing literature on the various applications of DECT, predominantly for abdominopelvic applications, showing potential for increased lesion conspicuity and improved tissue/material characterization.[4] Among the many other reported advantages include reduction of metallic artefacts,[5] number of phases of acquisition,[6] volume of contrast used,[7] and need for follow-up imaging.[8]

DECT has many promising applications in pancreatic imaging. Pancreatic pathologies are of great clinical significance, and yet are often subtle and difficult to detect on conventional CT. Many pancreatic lesions are detected incidentally during CT imaging for other reasons.[9] Furthermore, many pancreatic lesions are incompletely characterized on a conventional single portal venous phase acquisition and additional dedicated pancreatic CT and/or MRI are often necessary.[10] This presents an optimal target for application of dual energy technology to enable easier detection and better characterization of pancreatic pathology. This article reviews the current literature on the application of DECT for pancreatic pathologies and provides directions for future research.

DUAL ENERGY CT BASIC PRINCIPLES

Rather than imaging with a single polychromatic spectrum, DECT acquires data from two different X-ray spectra, generally low energy at 80 or 100 kVp and high energy at 140 kVp. CT-based material decomposition exploits the differences in X-ray absorption of materials as a function of X-ray energy; this allows materials with differential X-ray absorption at high and low kVp (*e.g.* calcium, iodine) to be directly quantified within images, or removed in post-processing. DECT can be acquired in multiple ways; two different X-ray tube sources and matching detector arrays at an approximately 90-degree offset that generate different energy beams (dual-source dual-energy); a single X-ray source that rapidly switches kVp to acquire two datasets near-simultaneously in interleaved projections; and a single X-ray source with a dual-layer detector that preferentially absorbs low and high energy X-rays in the surface and deep layers, respectively. Each method has distinct advantages and challenges.[11,12] Each system also employs slightly different dual energy post-processing techniques: dual-source DECT utilizes image-domain-based three-material decomposition (generally fat, soft tissue and iodine for abdominal applications and fat, soft tissue and calcium for osseous applications), while the rapid kVp switching and dual-layer detector approaches typically work in the projection domain using two material decomposition to create material density images.

Figure 1. A 45-year-old male with pancreatic adenocarcinoma. The "mixed" image (a) is a blended image that combines the low and high kVp datasets, to simulate a traditional 120 kVp image. Dual energy post-processing enables creation of VNC (b), iodine overlay (c) and VM images (d) shown here in the axial plane. Attenuation at various monoenergetic energy levels can be presented in a graphical format (e), displaying the expected CT attenuation values (*y*-axis) at varied X-ray energies in keV (*x*-axis), for the region of interest in the pancreatic tail (d). VM, virtual monoenergetic; VNC, virtual non-contrast.

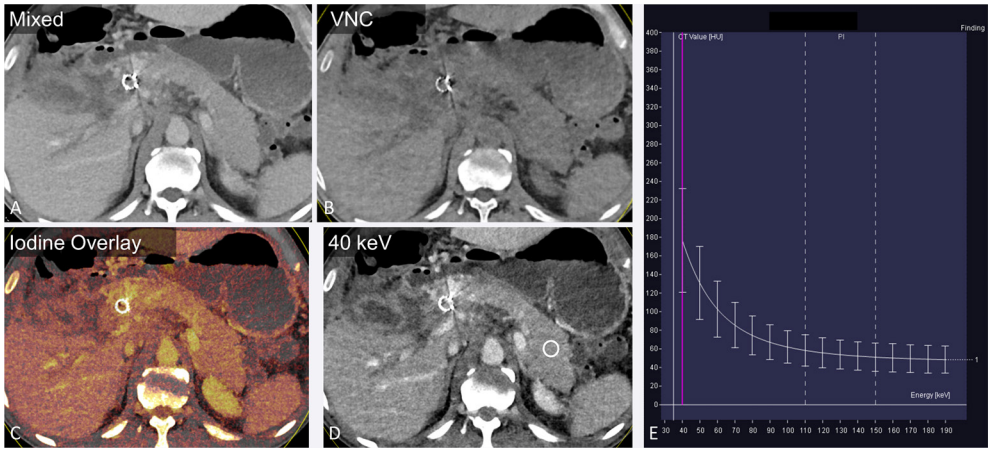

DUAL ENERGY CT IN PANCREATIC IMAGING: POST-PROCESSING TECHNIQUES

Regardless of the variations in post-processing techniques between vendors, each method enables creation of virtual non-contrast (VNC) and virtual monoenergetic (VM) images, as well as the assessment of enhancement through iodine maps.

Iodine selective imaging

Material decomposition-based iodine extraction enables generation of both VNC and iodine selective images (iodine overlay or iodine maps) from a dual energy acquisition (Figure 1). The VNC images offer the opportunity to avoid a separate non-contrast acquisition, while enabling differentiation of contrast from calcium or other dense material (ingested, iatrogenic or other foreign material). Iodine selective imaging can be displayed differently on specific post-processing softwares and enable both subjective and quantitative (both absolute and relative) determination of enhancement.

Although non-contrast imaging plays a small role in pancreatic imaging, there are many studies that have examined the image quality of VNC images in evaluating the pancreas and for other abdominal applications. VNC images created from a dual energy acquisition for pancreatic applications have been reported to have excellent image quality, with some studies reporting identical image quality to true non-contrast (TNC) imaging,[13,14] and others reporting slightly inferior image quality[15] (Figure 2). De Cecco et al in a study of 111 patients attributed this slightly inferior subjective image quality to blurred organ margins, likely due to imperfect fusion of the two image datasets.[15] However, all VNC images were considered acceptable as replacement for TNC images by both readers in this study.[15] Using the same dual energy system, Kaufman et al reported similar objective edge sharpness for VNC and TNC images.[16] Despite possible small differences in image quality, VNC images have been reported to be completely acceptable in ~91% cases.[14] Some studies have reported a decrease in image noise with VNC images,[13,16] which may be secondary to image filtering and post-processing that work to "smooth" the data.[6,14,17]

Good correlation has been reported between pancreatic HU measurements from TNC and VNC images;[16,18] the difference in HU although statistically different in the study by Kaufman et al was in the range of 1–5 HU[15,16] (Figure 2). These differences

Figure 2. A 45-year-old male with pancreatic adenocarcinoma status post-stent placement (same patient as in Figure 1). Axial VNC (a) and TNC (b, 120 kVp) images acquired within 10 days demonstrate similar pancreatic attenuation. The VNC image demonstrates slightly increased noise when compared with the TNC image. TNC, true non-contrast; VNC, virtual non-contrast.

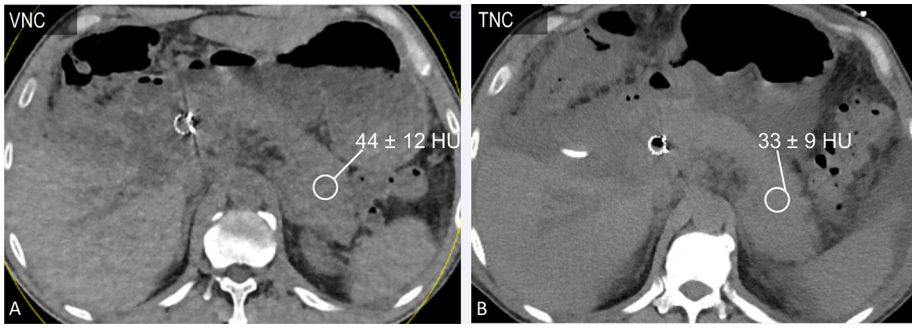

Figure 3. A 38-year-old male presenting with abdominal pain. Oblique coronal image demonstrates an ill-defined hypodensity in the pancreatic tail (a). The difference in enhancement relative to the pancreatic body is accentuated by the use of iodine overlay (b) and virtual monoenergetic imaging at 50 keV (c).

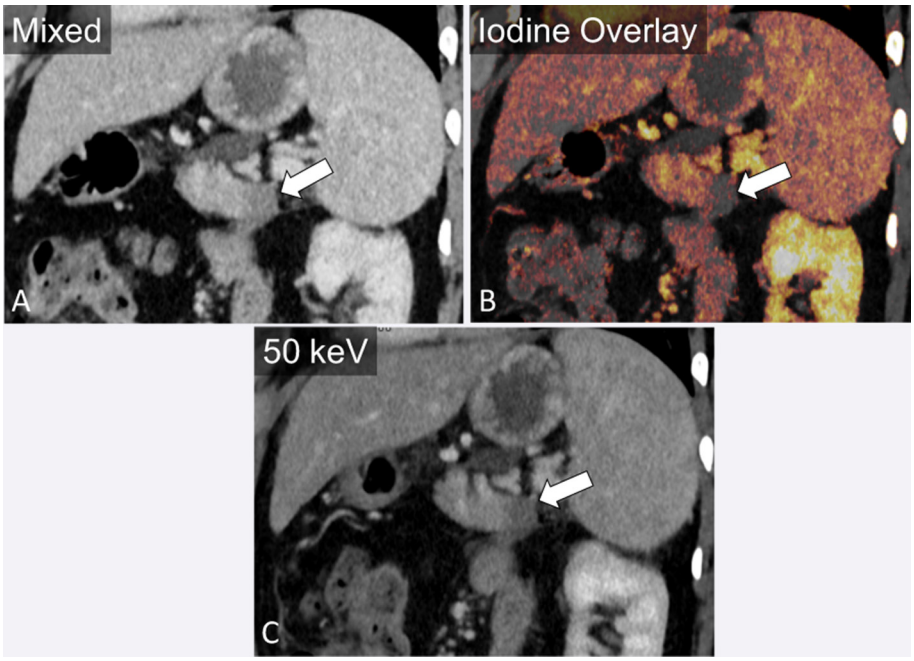

in pancreatic attenuation are small and within the range of variability in enhancement reported within the pancreatic parenchyma (head to tail; 2–31 HU (3–34%), and 24% variation in iodine concentration).[19]

Virtual monoenergetic imaging

Knowledge of the attenuation characteristics of tissues using two different polychromatic energy spectra also allows for creation of virtual monochromatic images at multiple simulated energy levels. These images enable accentuation of contrast enhancement by choosing an energy level close to the k-edge of iodine. The tissue attenuation across different energy levels can also be represented in a graphical format (Figure 1) for easy comparison of tissue properties and/or iodine content.

For general abdominal applications, VM images at 70 keV have been shown to have better objective and subjective image quality than 120 kVp images.[20] A lower energy level is often used for pancreatic applications with most of the reported studies using 50–70 keV VM images as the optimal energy for pancreatic imaging, as these lower energy levels accentuate subtle difference in iodine contrast enhancement (Figure 3).[21] When using a weight-based reduced contrast injection (average 37% contrast volume reduction), VM images at 52 keV were nonetheless found to have higher mean pancreatic parenchymal attenuation compared with conventional contrast volume at 120 kVp, without a change in CNR or image quality.[7]

DOSE REDUCTION

Conventional dedicated pancreatic imaging with CT commonly includes both a pancreatic phase (35–45 s, for better lesion conspicuity) and portal venous phase (60–70 s), while an arterial phase is often added for pre-surgical vascular evaluation.[22,23] When bolus tracking is employed, pancreatic phase imaging can be acquired using a 100 HU threshold in the descending aorta and a 35 s diagnostic delay.[24] Dual energy CT demonstrates potential in pancreatic imaging by enabling generation of VM low keV images to enhance contrast and iodine overlay images to better characterize enhancement from a single phase acquisition. This allows for potential dose reduction by avoiding multiple scan phases, and may also be used to decrease contrast usage.[13,25] Potential radiation dose reduction on the order of 14–27% has been reported with omission of a noncontrast acquisition for abdominopelvic imaging,[6,13–15] although this has limited applications in pancreatic imaging. In one study, a 57% radiation dose savings was observed by replacing a TNC with a "dose-free" VNC, and replacing a pancreatic phase acquisition with the high contrast 100 kVp half of the dual energy portal venous phase acquisition, thus reducing a three-phase acquisition to a single portal venous phase acquisition.[26]

PANCREATIC LESION DETECTION AND CHARACTERIZATION

A large proportion of focal pancreatic lesions are slightly hypo- to isodense to the pancreas on CT, rendering detection difficult. A large body of research has assessed the utility of low keV VM images in the diagnosis and characterization of pancreatic lesions. As would be expected, a higher contrast to noise ratio (CNR) of lesions has been reported at 55 keV monochromatic images compared with routine 120 kVp images with subjective reader preference of lower keV images in 70.1–95.8% cases for pancreatic applications.[27] Of note, in this study there was no difference noted in subjective lesion sharpness or visualization of internal structures.[27] Another approach is to use differential

weighting of the two acquisitions with an equal weighting of the high and low kVp acquisitions preferred for image quality, but a low-kVp weighted image being better for lesion conspicuity.[14] He et al has also reported a non-linear blending technique with the low HU values derived mostly from the high kVp dataset and the high HU values derived mostly from the low kVp dataset[24] for optimal CNR of pancreatic lesions. This is likely reflective of a combination of the optimal contrast achieved at low kVp with the optimal low noise of a high kVp dataset. Higher attenuation difference between focal pancreatic lesions and the parenchyma has been noted at 52 keV, even using a 37% average lower contrast dose, as compared with 120 kVp.[7] A dual energy-based approach (VNC and 100 kVp images acquired in portal venous phase replacing the TNC and 120 kVp pancreatic phase, in addition to the fused 120 kVp portal venous phase for both approaches) has been demonstrated to have sufficient image quality, similar diagnostic accuracy and better diagnostic confidence[26] for pancreatic lesions.

Pancreatic Adenocarcinoma

Pancreatic adenocarcinoma is characteristically hypovascular due to associated desmoplasia and fibrosis.[25] Many studies have specifically evaluated imaging of pancreatic adenocarcinoma with DECT. Early studies on pancreatic adenocarcinoma showed that images from the low energy (80 or 100 kVp) portion of the DECT acquisition had higher attenuation differences relative to normal parenchyma,[26] higher CNR and subjectively better tumour conspicuity and duct visualization compared with the 140 kVp or weighted average 120 kVp images,[28,29] although increased image noise was noted in the low kVp images.

Many studies have evaluated VM imaging in pancreatic tumour evaluation. Early studies showed that the energy level for optimal CNR and signal to noise ratio was 50–74 keV in the pancreatic phase of acquisition[24,30] (Figure 3). Some studies have demonstrated 70 keV to be qualitatively best[31,32] to identify tumour extension and vascular invasion, with more than half of the 50 keV and 60 keV images rated poor to markedly limited.[31] However, novel noise-optimized monoenergetic reconstruction algorithms are now available to reduce the noise previously observed at lower keV. Using these algorithms, peak CNR is achieved at 40 keV and 55–65 keV is preferred for overall image quality.[33,34] In another study employing DECT in both pancreatic and portal venous phases, the CNR was highest at 61–74 keV for the pancreatic phase and 68–86 keV for the portal venous phase, which was higher than the CNR for the corresponding weighted average 120 kVp equivalent images.[35] Within the optimal monoenergetic images, the pancreatic phase had higher CNR compared with the portal venous phase.[35] Similarly, Yin et al, while reconstructing VM images at 10 keV increments, reported a higher CNR for pancreatic adenocarcinoma at 40–70 keV in arterial and portal venous phases[36] when compared with 80–140 keV. Moreover, iodine material density images have been demonstrated to have the highest SNR and CNR compared with both monochromatic and conventional 120 kVp images for pancreatic adenocarcinoma and have also been rated qualitatively best for primary tumour visualization and reader confidence.[31,32]

The iodine-only images have been shown to add value in ~50% cases of pancreatic tumour,[14] with reported reasons including more reliable determination of solid *vs* cystic nature, better lesion conspicuity, and evaluation of the relationship of pancreatic duct to adjacent vessels.[14]

Furthermore, comparison of tumour dimensions on low keV and iodine map images to polychromatic 140 kVp images have yielded similar values.[21] Beyond detection and measurement of adenocarcinoma, DECT also offers potential advantages in assessment of vascular invasion by augmenting vascular enhancement using low keV VM images (Figure 4).[37] In addition, dual energy-based metal reduction algorithms could also help reduce artefact around surgical clips or bile duct stents.[38]

Pancreatic adenocarcinomas are known to demonstrate low blood flow and blood volume relative to the normal pancreatic parenchyma on perfusion imaging.[35] Perfusion imaging is also feasible with dual energy CT[19] with the mixed 120 kVp images demonstrating smaller standard deviations in perfusion values compared with 80 and 140 kVp source images.[39] Moreover, acceptable-to good correlation (correlation coefficient of 0.56 and 0.89 for normal pancreas and pancreatic adenocarcinoma, respectively) has been found between perfusion values from a dynamic acquisition and iodine concentration derived from a single dual energy acquisition at 32 s from contrast injection.[40]

It is important to note that despite improvements in image quality and diagnostic confidence demonstrated with DECT, there is no proven increase in tumour detection with application of low kVp or low keV VM images.[26,29] Further research is needed to determine if low kVp or keV imaging can truly improve lesion detection.

Another demonstrated benefit of DECT is in the differentiation of adenocarcinoma from chronic mass-forming pancreatitis. These two entities are challenging to distinguish even on histopathology, and the reported incidence of chronic inflammatory disease in patients undergoing Whipple procedure for clinically suspected pancreatic cancer is up to 13%.[41] An area under the receiver operating curve in the range of 0.97–0.98 has been reported to differentiate between these pathologies by using the lesion iodine concentration normalized to the iodine concentration in the aorta, and the K slope of the monoenergetic CT values defined as $|CT_{(90\ keV)} - CT_{(40\ keV)}|/50$.[36] The normalized iodine concentration and K slope were higher for chronic mass-forming pancreatitis compared with adenocarcinoma on both arterial and portal venous phase images (mean NIC 0.26 *vs* 0.07 on arterial phase and 0.53 *vs* 0.28 on portal venous phase; mean K slope 3.27 *vs* 1.35 on arterial phase and 3.7 *vs* 2.16 on portal venous phase)[36] (Figures 5 and 6).

Cystic pancreatic lesions

Cystic pancreatic lesions are an often encountered pancreatic pathology. VM imaging and iodine maps may better

Figure 4. A 45-year-old male with invasive pancreatic adenocarcinoma. Axial and coronal portal venous phase mixed images (a, c) demonstrate tumour encasing the superior mesenteric artery (block arrow) and superior mesenteric vein (SMV, dashed arrow) and occluding the portal vein (curved arrow) at the SMV/splenic vein confluence. Virtual monoenergetic images at 50 keV accentuate the iodinated contrast in the vasculature (b, d), improving assessment of vascular involvement.

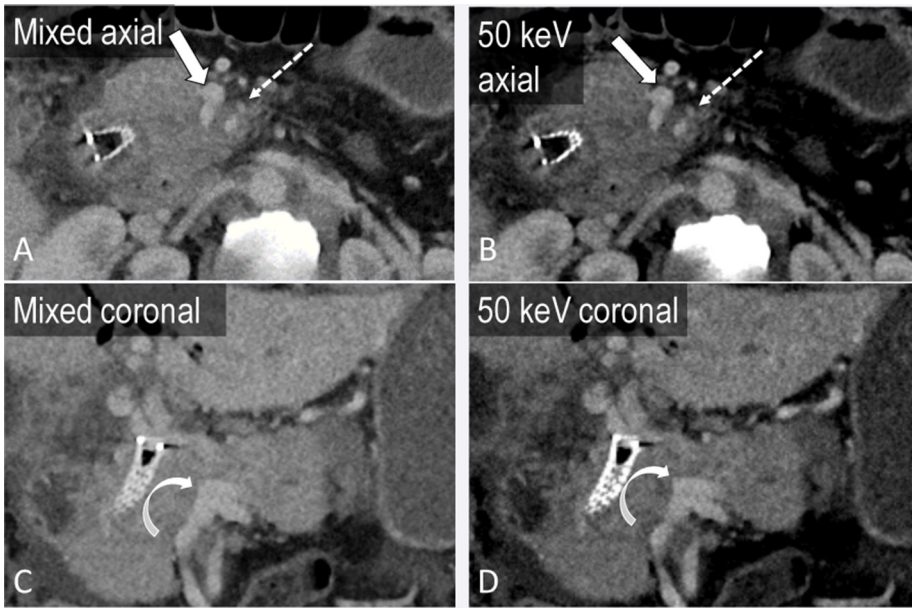

demonstrate the complexity of cystic masses[14,38] (Figures 7–9). Chu et al, while assessing 44 patients with focal pancreatic disease, found iodine-only images added value to determine the solid *vs* cystic nature of a lesion and improved lesion conspicuity, while also improving evaluation of the relationship of the tumour with the pancreatic duct and nearby vessels. Moreover, the differentiation of serous and mucinous cystic lesions, an important management distinction, has largely relied on additional imaging such as MRI.[42] Using DECT, monoenergetic attenuation and iodine density have been explored as factors to distinguish between serous and mucinous cystic lesions of the pancreas. High arterial phase attenuation at 40 keV (optimal cutoff > 35.7 HU) and arterial phase iodine density (optimal cutoff > 0.325 mg ml^{-1}) were found to be predictive of a mucinous cystic neoplasm with an AUC of 0.74 and 0.68, respectively, in addition to conventional

Figure 5. A 57-year-old male presenting with left lower quadrant pain. Mixed axial image from portal venous phase dual energy CT demonstrates subtle ill-defined hypodensity in the pancreatic body (a, arrow). The difference in enhancement is accentuated by the use of virtual monoenergetic images at 50 keV (b). The hypoenhancement of the pancreatic mass is also apparent on the iodine overlay images (c, arrow). Multiple hepatic metastases (dashed arrows) are also more apparent on the low keV image (b). The mass demonstrates a normalized iodine concentration (normalized to aorta) of 0.02 and slope K of the spectral curve of 0.11.

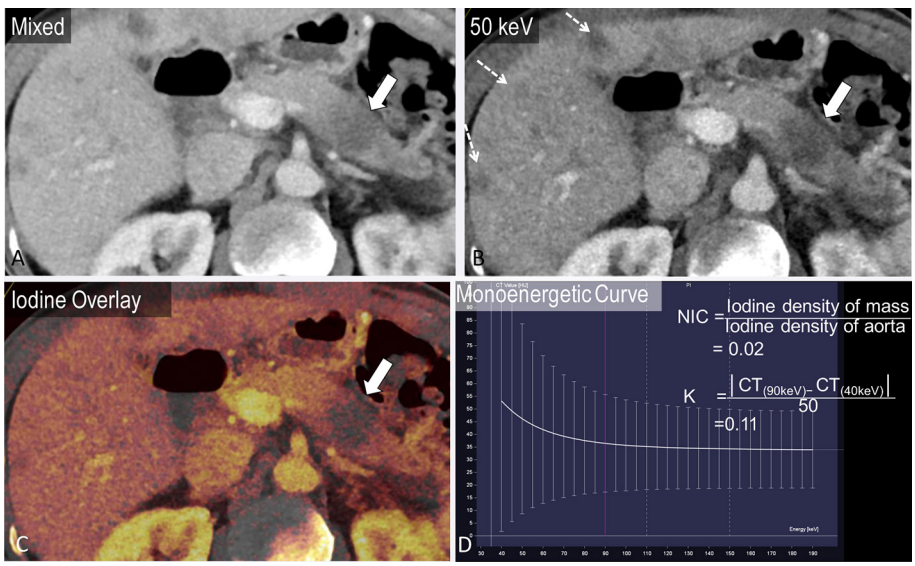

Figure 6. A 86-year-old male presenting with abdominal distention found to have ill-defined soft tissue at the uncinate process of the pancreas with surrounding stranding (a, axial image, block arrow), with atrophy of the pancreatic body and tail (b, dashed arrow). The differential diagnosis includes pancreatitis and pancreatic mass. The lesion demonstrates iodine content (NIC = 0.46 and K = 2.4), suggestive of mass-forming pancreatitis rather than pancreatic adenocarcinoma (c, f, contrast to Figure 5). MRI demonstrated T2 hyperintensity and enhancement, thought to be autoimmune pancreatitis, considering the waxing and waning masslike appearance over time (d, e).

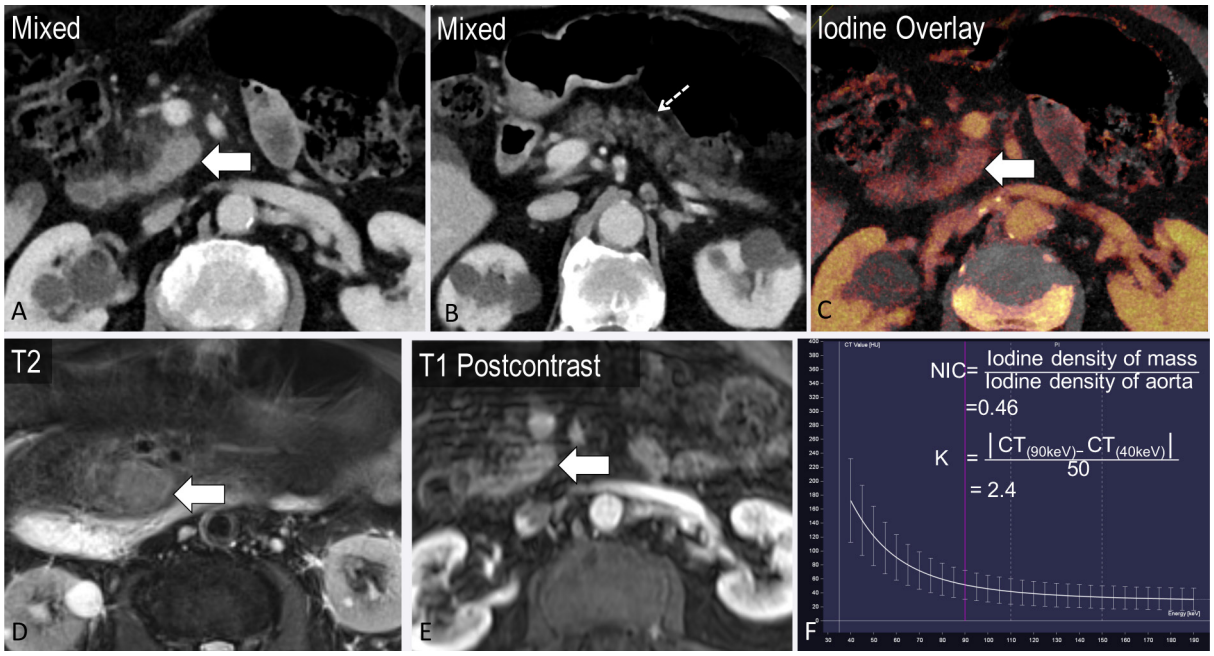

factors such as size and location.[43] For these two parameters, sensitivity was in the range of 89.4–94.7% and specificity was 56.5%.[43] In this study, a computer-aided diagnosis algorithm employing a set of conventional and dual-energy-based data successfully classified 93% cases of serous and mucinous tumours.[43]

Figure 7. Incidental finding in a 22-year-old presenting with epigastric pain. Ill-defined hypodense lesion in the pancreatic body on axial images (a, arrow) with iodine overlay demonstrating internal enhancing septations (b, dashed arrow). MRI shows internal T2 hyperintensity (c) and an enhancement pattern (d) similar to that seen on the iodine overlay; this was presumed to be a serous cystadenoma.

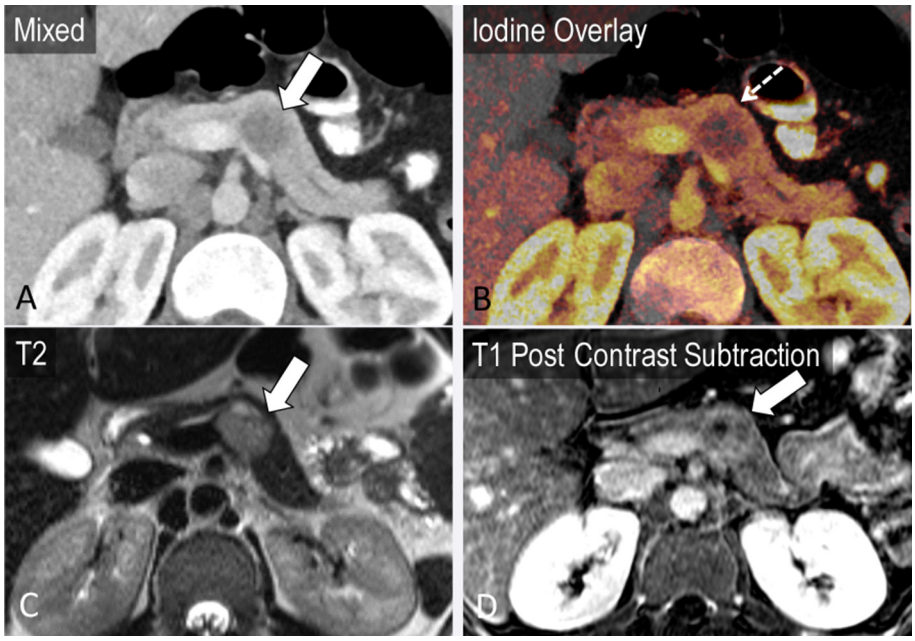

Figure 8. Incidental finding in an 85-year-old presenting with right lower quadrant pain. Cystic pancreatic lesion with internal septations on axial images (a, arrow), which are better seen on the 50 keV image (b). Subtle wall enhancement demonstrated on the iodine overlay image (c) corresponds to that on the post-contrast subtraction MRI (e).

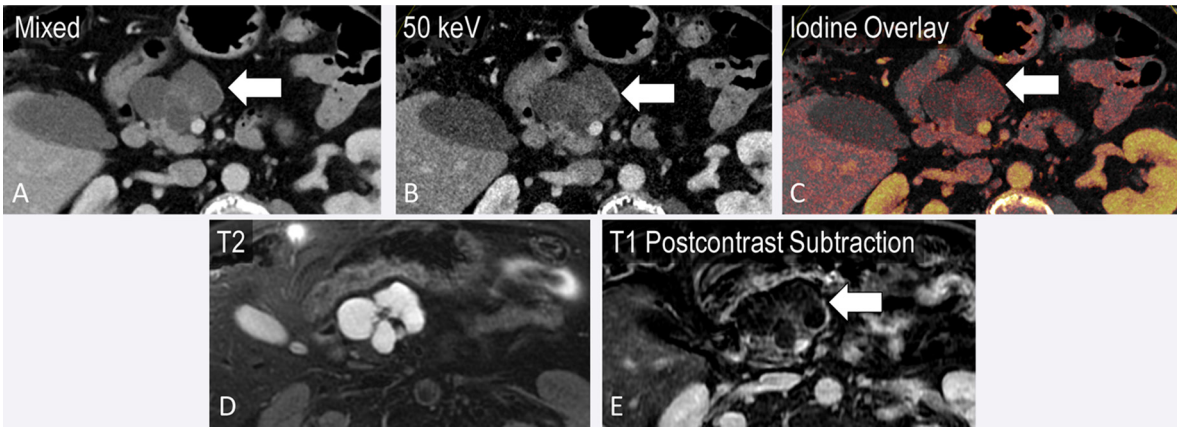

Other masses

There is limited data assessing the utility of dual energy CT for other pancreatic masses. Potential benefits include the evaluation of enhancement in neuroendocrine tumours (Figures 10 and 11),[44,45] hyper- or hypo-vascular metastases, and other incidental lesions such as intrapancreatic splenules (Figure 12). DECT (using a combination of monochromatic and iodine density imaging) has been shown to have a higher sensitivity for the detection of pancreatic insulinomas compared to conventional CT (95.7 *vs.* 68.8%) in a small study of 35 patients.[46]

PANCREATITIS

The utility of dual energy CT in pancreatitis is largely in the setting of complications such as necrosis, vascular complications and pancreatic/peripancreatic collections (Figures 13 and 14). Evaluation at a lower energy of 80 kVp has been reported to accentuate the difference in attenuation between the necrotic area and normal pancreas, thereby improving CNR, subjective assessment of necrosis and accentuating areas of hypovascularity around the necrosis.[47,48] Low keV images by enhancing contrast enhancement may improve the assessment of vascular complications such as thrombosis or pseudoaneurysm formation. Dual energy CT can also be used to assess the complexity of pancreatic/peripancreatic collections and to assess for residual enhancing parenchyma. VM images at high and low keV are also beneficial in the identification of non-calcified gallstones as a potential cause of pancreatitis[49,50] (Figure 15). Partial calcium subtraction may however limit the evaluation of chronic pancreatitis on VNC images.

Figure 9. A 25-year-old female with incidental finding after presentation for fall. A partially cystic mass in the tail of the pancreas is noted on mixed axial images from portal venous phase CT (a, block arrow). Iodine overlay images demonstrate nodular enhancement within the mass (b). T2 (c) and T1 post-contrast MRI images (d) confirm a cystic mass with areas of nodular enhancement corresponding to the iodine overlay images, most likely a pancreatic solid pseudopapillary epithelial neoplasm.

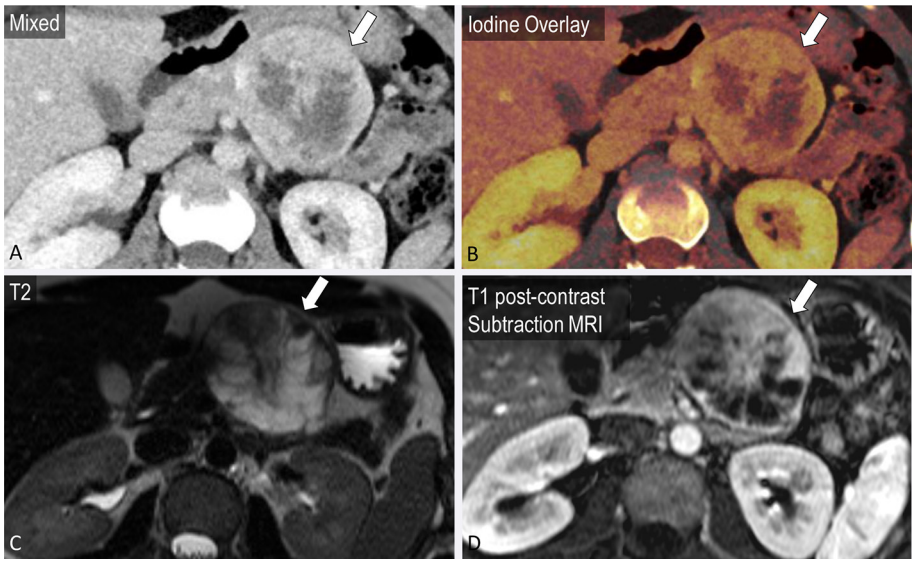

Figure 10. A 45-year-old female with known pancreatic neuroendocrine tumour. Mixed coronal image (a) demonstrates an enhancing exophytic mass arising from the body of the pancreas. Iodine overlay coronal and axial images (b, c) demonstrate an enhancing mass (arrow) and enhancing peritoneal metastatic deposits (dashed arrow).

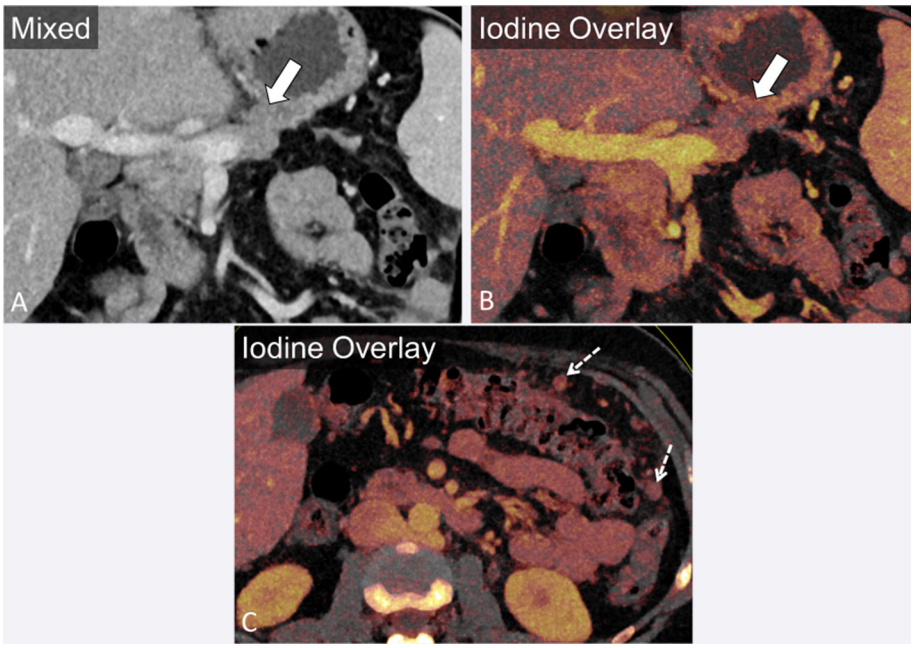

IMAGE ARTEFACTS AND DIAGNOSTIC PITFALLS

Various image artefacts unique to dual-energy post-processed images have been reported.[14] For example, subtraction-related artefacts may occur including blurring due to motion/inadequate breath hold, partial subtraction of calcifications/hardware,[13–15] and incomplete iodine subtraction.[13,15] It is important to recognize that on a dual-source scanner, due to the 90-degree offset between tubes, motion artefacts may be imaged differently by the two tubes and hence their effect on the mixed images and the VNC images can be different, which may rarely mimic pathology.[6] Using a second-generation dual energy scanner, De Cecco et al reported higher pancreatic parenchymal attenuation on VNC images generated from arterial and portal venous phase acquisition as opposed to the TNC images.[15] This is likely due to incomplete iodine subtraction; supported by the higher attenuation of arterially enhancing organs on the VNC images generated

Figure 11. A 32-year-old female presenting with nausea, vomiting and epigastric pain. Mixed coronal image (a) demonstrates a mass in the neck of the pancreas, hyperenhancing relative to the body, with associated pancreatic ductal dilatation. Iodine overlay images can quantify the degree of enhancement as greater than double that of the normal pancreatic parenchyma (b, c). Biopsy confirmed a pancreatic neuroendocrine tumour.

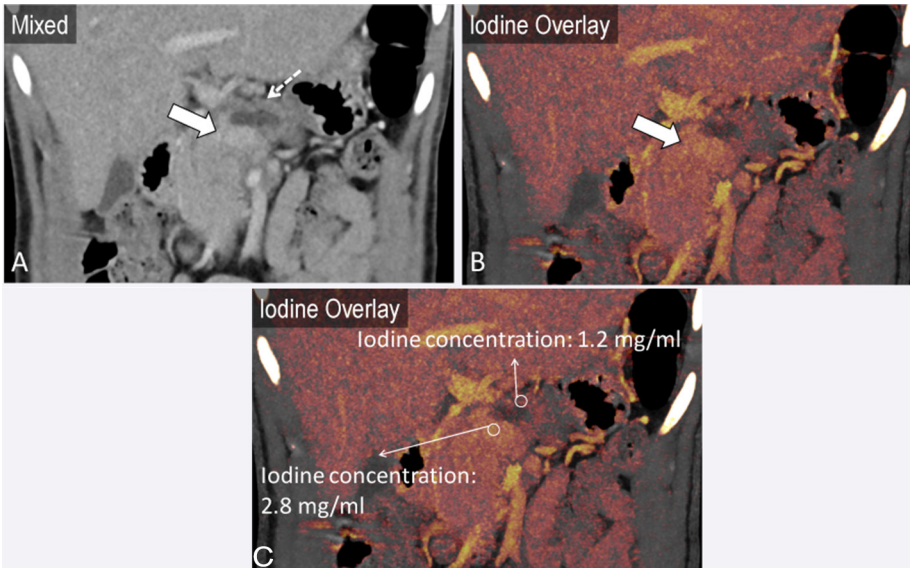

Figure 12. A 77-year-old female with incidental finding after presentation for fever. A solid enhancing mass is seen in the pancreatic tail (a, arrow). 60 keV and axial iodine overlay images demonstrate similarity in attenuation and iodine content to the spleen (b, c, dashed arrow). The mass has an identical monoenergetic HU spectrum when compared with the spleen (e). Contrast enhanced MRI demonstrates similarity in intensity to the spleen (d) on all sequences, confirming an intrapancreatic splenule.

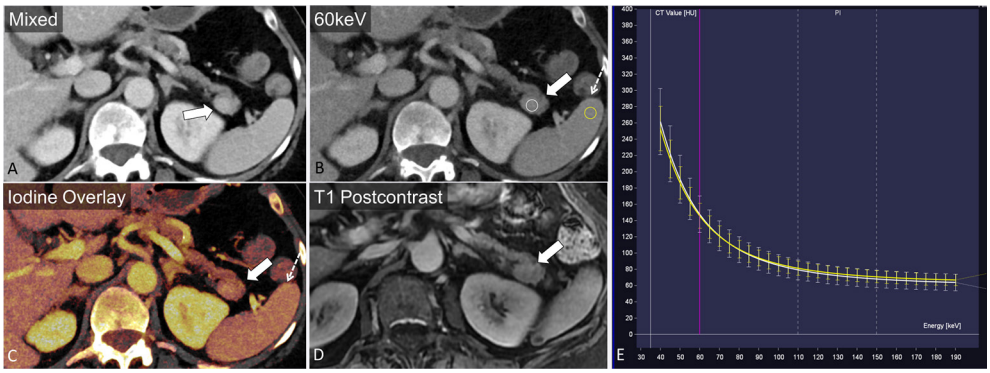

from the arterial phase scan as opposed to the higher attenuation of organs that enhance in the portal venous phase, such as the liver, on the VNC images generated from the portal venous phase acquisition.[15] The artefact related to inaccurate subtraction has also been manifested in the liver, where higher detection of hypodense hepatic lesions and lower detection of small calcified hepatic lesions have been reported on VNC images (from arterial and portal venous phase acquisition) compared to TNC images.[15]

Although the smaller field of view of the second X-ray tube was a limitation of the first-generation scanner which has been overcome with newer generation scanners, this is generally not of concern in the evaluation of centrally located pancreas in even large patients. However, the single source rapid kVp switching system cannot generally be used in patients > 250 lbs due to limited penetration of the 80 kVp beam.

FUTURE DIRECTIONS

While there are many studies on the improved subjective and objective image quality, reader preference and diagnostic confidence associated with dual energy post-processed images, diagnostic yield and accuracy of detection of pancreatic lesions (particularly adenocarcinoma) need to be established. There is a vast amount of information on lesion heterogeneity, vascularity, and material properties that can be extracted from dual-energy

Figure 13. A 45-year-old male presenting with abdominal pain. Fat stranding surrounding the pancreatic head suggests pancreatitis (a). Axial iodine overlay and monoenergetic images at 50 keV accentuate enhancement differences in the pancreatic head (b, c). Quantification of contrast enhancement enables detection of a subtle area of decreased enhancement (CT attenuation: 25.9 HU and iodine concentration: 1.0 mg ml^{-1}) in the pancreatic head, relative to the normal uncinate process (CT attenuation: 51.1 HU and iodine concentration: 2.2 mg ml^{-1}), suggestive of necrosis.

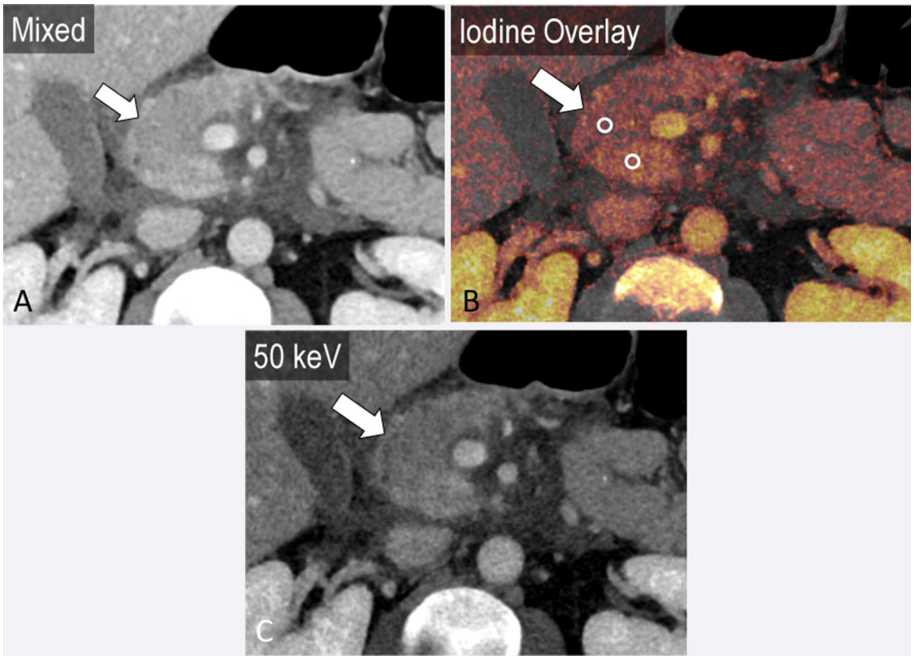

Figure 14. A 40-year-old male presenting with diffuse abdominal pain diagnosed with pancreatitis (a). Axial monoenergetic image at 50 keV and iodine overlay accentuate the lack of enhancement of the pancreatic tail indicating necrosis (b, c).

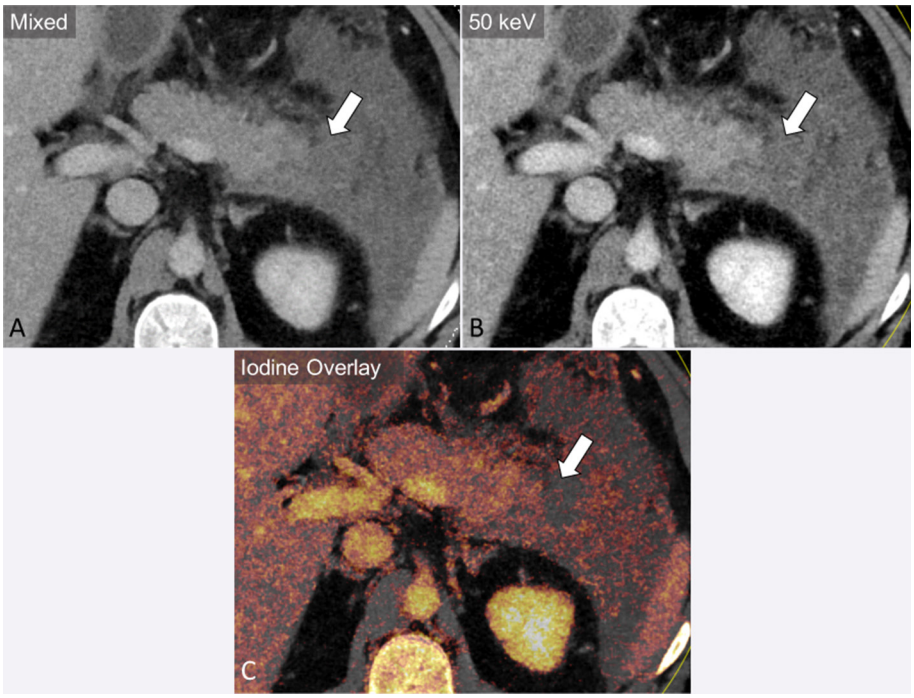

post-processing; further research is needed to correlate these findings with imaging findings on other modalities, such as MRI and PET,[51] as well as to evaluate the correlation between DECT imaging features and prognosis. Other potential research opportunities include differentiation of true neoplastic tissue from desmoplastic reaction in pancreatic adenocarcinoma, as has been attempted with MRI.[52] Similarly, in the evaluation of cystic pancreatic lesions, systematic studies comparing lesion characterization on DECT and MRI are required to assess the accuracy and potential benefit of avoidance of additional imaging. In cases of pancreatitis, while necrosis is a late finding on conventional CT, the benefits on DECT for early detection and prediction of clinical outcome also need to be further explored.

CONCLUSION

Dual energy post-processing offers many advantages over conventional CT in the evaluation of pancreatic pathologies, including better image quality in the detection and local staging of pancreatic

Figure 15. Incidental finding in a 65-year-old female patient. Relatively homogenous appearance of the gallbladder on mixed axial images (a). Monoenergetic axial images at 40 keV and 190 keV enable visualization of layering gallstones (b, c), confirmed on MRI (d).

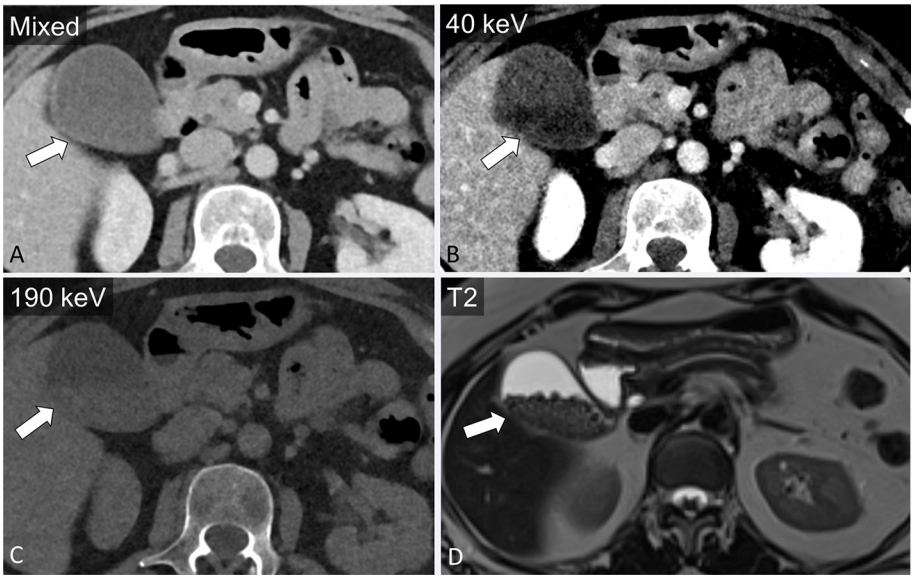

adenocarcinoma, differentiation of adenocarcinoma from mass-forming pancreatitis, characterization of other pancreatic pathologies including cystic lesions, and for assessment of complications of pancreatitis. DECT also offers promise in decreasing the number of phases of acquisition for potential dose reduction and for reduced volume contrast usage. Future studies are necessary to further establish the diagnostic accuracy and specific clinical and prognostic advantages of this alternative imaging method.

FUNDING

Dr. Sodickson received research funding from Siemens AG.

REFERENCES

1. Rutherford RA, Pullan BR, Isherwood I. X-ray energies for effective atomic number determination. *Neuroradiology* 1976; **11**: 23–8. doi: https://doi.org/10.1007/BF00327254
2. Rutherford RA, Pullan BR, Isherwood I. Measurement of effective atomic number and electron density using an EMI scanner. *Neuroradiology* 1976; **11**: 15–21. doi: https://doi.org/10.1007/BF00327253
3. Millner MR, McDavid WD, Waggener RG, Dennis MJ, Payne WH, Sank VJ. Extraction of information from CT scans at different energies. *Med Phys* 1979; **6**: 70–1. doi: https://doi.org/10.1118/1.594555
4. Heye T, Nelson RC, Ho LM, Marin D, Boll DT. Dual-energy CT applications in the abdomen. *AJR Am J Roentgenol* 2012; **199**(5 Suppl. 5): S64–70S70. doi: https://doi.org/10.2214/AJR.12.9196
5. Pessis E, Sverzut JM, Campagna R, Guerini H, Feydy A, Drapé JL. Reduction of metal artifact with dual-energy CT: virtual monospectral imaging with fast kilovoltage switching and metal artifact reduction software. *Semin Musculoskelet Radiol* 2015; **19**: 446–55. doi: https://doi.org/10.1055/s-0035-1569256
6. Barrett T, Bowden DJ, Shaida N, Godfrey EM, Taylor A, Lomas DJ, et al. Virtual unenhanced second generation dual-source CT of the liver: is it time to discard the conventional unenhanced phase? *Eur J Radiol* 2012; **81**: 1438–45. doi: https://doi.org/10.1016/j.ejrad.2011.03.042
7. Clark ZE, Bolus DN, Little MD, Morgan DE. Abdominal rapid-kVp-switching dual-energy MDCT with reduced IV contrast compared to conventional MDCT with standard weight-based IV contrast: an intra-patient comparison. *Abdom Imaging* 2015; **40**: 852–8. doi: https://doi.org/10.1007/s00261-014-0253-3
8. Wortman JR, Bunch PM, Fulwadhva UP, Bonci GA, Sodickson AD. Dual-energy CT of incidental findings in the abdomen: can we reduce the need for follow-up imaging? *AJR Am J Roentgenol* 2016; **207**: W58–W68. doi: https://doi.org/10.2214/AJR.16.16087
9. Laffan TA, Horton KM, Klein AP, Berlanstein B, Siegelman SS, Kawamoto S, et al. Prevalence of unsuspected pancreatic cysts on MDCT. *AJR Am J Roentgenol* 2008; **191**: 802–7. doi: https://doi.org/10.2214/AJR.07.3340
10. Foley WD, Kerimoglu U. Abdominal MDCT: liver, pancreas, and biliary tract. *Semin Ultrasound CT MR* 2004; **25**: 122–44. doi: https://doi.org/10.1016/j.sult.2003.12.001
11. Kaza RK, Platt JF, Cohan RH, Caoili EM, Al-Hawary MM, Wasnik A. Dual-energy CT with single- and dual-source scanners: current applications in evaluating the genitourinary tract. *Radiographics* 2012; **32**: 353–69. doi: https://doi.org/10.1148/rg.322115065
12. McCollough CH, Leng S, Yu L, Fletcher JG. Dual- and Multi-Energy CT: Principles, Technical Approaches, and Clinical Applications. *Radiology* 2015; **276**: 637–53. doi: https://doi.org/10.1148/radiol.2015142631
13. Mileto A, Mazziotti S, Gaeta M, Bottari A, Zimbaro F, Giardina C, et al. Pancreatic dual-source dual-energy CT: is it time to discard unenhanced imaging? *Clin Radiol* 2012; **67**: 334–9. doi: https://doi.org/10.1016/j.crad.2011.09.004
14. Chu AJ, Lee JM, Lee YJ, Moon SK, Han JK, Choi BI. Dual-source, dual-energy multidetector CT for the evaluation of pancreatic tumours. *Br J Radiol* 2012; **85**: e891–8e898. doi: https://doi.org/10.1259/bjr/26129418
15. De Cecco CN, Darnell A, Macías N, Ayuso JR, Rodríguez S, Rimola J, et al. Virtual unenhanced images of the abdomen with second-generation dual-source dual-energy computed tomography: image quality and liver lesion detection. *Invest Radiol* 2013; **48**: 1–9. doi: https://doi.org/10.1097/RLI.0b013e31826e7902
16. Kaufmann S, Sauter A, Spira D, Gatidis S, Ketelsen D, Heuschmid M, et al. Tin-filter enhanced dual-energy-CT: image quality and accuracy of CT numbers in virtual noncontrast imaging. *Acad Radiol* 2013; **20**: 596–603. doi: https://doi.org/10.1016/j.acra.2013.01.010
17. Graser A, Johnson TR, Hecht EM, Becker CR, Leidecker C, Staehler M, et al. Dual-energy CT in patients suspected of having renal masses: can virtual nonenhanced images replace true nonenhanced images? *Radiology* 2009; **252**: 433–40. doi: https://doi.org/10.1148/radiol.2522080557
18. Borhani AA, Kulzer M, Iranpour N, Ghodadra A, Sparrow M, Furlan A, et al. Comparison of true unenhanced and virtual unenhanced (VUE) attenuation values in abdominopelvic single-source rapid kilovoltage-switching spectral CT. *Abdom Radiol* 2017; **42**: 710–7. doi: https://doi.org/10.1007/s00261-016-0991-5
19. Delrue L, Blanckaert P, Mertens D, De Waele J, Ceelen W, Achten E, et al. Variability of CT contrast enhancement in the pancreas: a cause for concern? *Pancreatology* 2011; **11**: 588–94. doi: https://doi.org/10.1159/000334547
20. Yamada Y, Jinzaki M, Hosokawa T, Tanami Y, Abe T, Kuribayashi S. Abdominal CT: an intra-individual comparison between virtual monochromatic spectral and polychromatic 120-kVp images obtained during the same examination. *Eur J Radiol* 2014; **83**: 1715–22. doi: https://doi.org/10.1016/j.ejrad.2014.06.004
21. Gupta S, Wagner-Bartak N, Jensen CT, Hui A, Wei W, Lertdilok P, et al. Dual-energy CT of pancreatic adenocarcinoma: reproducibility of primary tumor measurements and assessment of tumor conspicuity and margin sharpness. *Abdom Radiol* 2016; **41**: 1317–24. doi: https://doi.org/10.1007/s00261-016-0689-8
22. Gilbert JW, Wolpin B, Clancy T, Wang J, Mamon H, Shinagare AB, et al. Borderline resectable pancreatic cancer: conceptual evolution and current approach to image-based classification. *Ann Oncol* 2017; **28**: 2067-2076. doi: https://doi.org/10.1093/annonc/mdx180
23. Small W, Hayes JP, Suh WW, Abdel-Wahab M, Abrams RA, Azad N, et al. ACR

appropriateness criteria® borderline and unresectable pancreas cancer. *Oncology* 2016; **30**: 619–24.
24. He YL, Zhang DM, Xue HD, Jin ZY. Clinical value of dual-energy CT in detection of pancreatic adenocarcinoma: investigation of the best pancreatic tumor contrast to noise ratio. *Chin Med Sci J* 2013; **27**: 207–12.
25. Graser A, Johnson TR, Chandarana H, Macari M. Dual energy CT: preliminary observations and potential clinical applications in the abdomen. *Eur Radiol* 2009; **19**: 13–23. doi: https://doi.org/10.1007/s00330-008-1122-7
26. Quiney B, Harris A, McLaughlin P, Nicolaou S. Dual-energy CT increases reader confidence in the detection and diagnosis of hypoattenuating pancreatic lesions. *Abdom Imaging* 2015; **40**: 859–64. doi: https://doi.org/10.1007/s00261-014-0254-2
27. Hardie AD, Picard MM, Camp ER, Perry JD, Suranyi P, De Cecco CN, et al. Application of an Advanced Image-Based Virtual Monoenergetic Reconstruction of Dual Source Dual-Energy CT Data at Low keV Increases Image Quality for Routine Pancreas Imaging. *J Comput Assist Tomogr* 2015; **39**: 716–20. doi: https://doi.org/10.1097/RCT.0000000000000276
28. Macari M, Spieler B, Kim D, Graser A, Megibow AJ, Babb J, et al. Dual-source dual-energy MDCT of pancreatic adenocarcinoma: initial observations with data generated at 80 kVp and at simulated weighted-average 120 kVp. *AJR Am J Roentgenol* 2010; **194**: W27–32W32. doi: https://doi.org/10.2214/AJR.09.2737
29. Marin D, Nelson RC, Barnhart H, Schindera ST, Ho LM, Jaffe TA, et al. Detection of pancreatic tumors, image quality, and radiation dose during the pancreatic parenchymal phase: effect of a low-tube-voltage, high-tube-current CT technique – preliminary results. *Radiology* 2010; **256**: 450–9. doi: https://doi.org/10.1148/radiol.10091819
30. Patel BN, Thomas JV, Lockhart ME, Berland LL, Morgan DE. Single-source dual-energy spectral multidetector CT of pancreatic adenocarcinoma: optimization of energy level viewing significantly increases lesion contrast. *Clin Radiol* 2013; **68**: 148–54. doi: https://doi.org/10.1016/j.crad.2012.06.108
31. Bhosale P, Le O, Balachandran A, Fox P, Paulson E, Tamm E. Quantitative and qualitative comparison of single-source dual-energy computed tomography and 120-kVp computed tomography for the assessment of pancreatic ductal adenocarcinoma. *J Comput Assist Tomogr* 2015; **39**: 907–13. doi: https://doi.org/10.1097/RCT.0000000000000295
32. McNamara MM, Little MD, Alexander LF, Carroll LV, Beasley TM, Morgan DE. Multireader evaluation of lesion conspicuity in small pancreatic adenocarcinomas: complimentary value of iodine material density and low keV simulated monoenergetic images using multiphasic rapid kVp-switching dual energy CT. *Abdom Imaging* 2015; **40**: 1230–40. doi: https://doi.org/10.1007/s00261-014-0274-y
33. Frellesen C, Fessler F, Hardie AD, Wichmann JL, De Cecco CN, Schoepf UJ, et al. Dual-energy CT of the pancreas: improved carcinoma-to-pancreas contrast with a noise-optimized monoenergetic reconstruction algorithm. *Eur J Radiol* 2015; **84**: 2052–8. doi: https://doi.org/10.1016/j.ejrad.2015.07.020
34. Bellini D, Gupta S, Ramirez-Giraldo JC, Fu W, Stinnett SS, Patel B, et al. Use of a Noise Optimized Monoenergetic Algorithm for Patient-Size Independent Selection of an Optimal Energy Level During Dual-Energy CT of the Pancreas. *J Comput Assist Tomogr* 2017; **41**: 39–47. doi: https://doi.org/10.1097/RCT.0000000000000492
35. Li HO, Guo J, Sun C, Li X, Qi YD, Wang XM, et al. Assessment of pancreatic adenocarcinoma: Use of low-dose whole pancreatic CT perfusion and individualized dual-energy CT scanning. *J Med Imaging Radiat Oncol* 2015; **59**: 590–8. doi: https://doi.org/10.1111/1754-9485.12342
36. Yin Q, Zou X, Zai X, Wu Z, Wu Q, Jiang X, et al. Pancreatic ductal adenocarcinoma and chronic mass-forming pancreatitis: Differentiation with dual-energy MDCT in spectral imaging mode. *Eur J Radiol* 2015; **84**: 2470–6. doi: https://doi.org/10.1016/j.ejrad.2015.09.023
37. Albrecht MH, Scholtz JE, Hüsers K, Beeres M, Bucher AM, Kaup M, et al. Advanced image-based virtual monoenergetic dual-energy CT angiography of the abdomen: optimization of kiloelectron volt settings to improve image contrast. *Eur Radiol* 2016; **26**: 1863–70. doi: https://doi.org/10.1007/s00330-015-3970-2
38. Morgan DE. Dual-energy CT of the abdomen. *Abdom Imaging* 2014; **39**: 108–34. doi: https://doi.org/10.1007/s00261-013-0033-5
39. Klauss M, Stiller W, Pahn G, Fritz F, Kieser M, Werner J, et al. Dual-energy perfusion-CT of pancreatic adenocarcinoma. *Eur J Radiol* 2013; **82**: 208–14. doi: https://doi.org/10.1016/j.ejrad.2012.09.012
40. Stiller W, Skornitzke S, Fritz F, Klauss M, Hansen J, Pahn G, et al. Correlation of quantitative dual-energy computed tomography iodine maps and abdominal computed tomography perfusion measurements: are single-acquisition dual-energy computed tomography iodine maps more than a reduced-dose surrogate of conventional computed tomography perfusion? *Invest Radiol* 2015; **50**: 703–8. doi: https://doi.org/10.1097/RLI.0000000000000176
41. Kennedy T, Preczewski L, Stocker SJ, Rao SM, Parsons WG, Wayne JD, et al. Incidence of benign inflammatory disease in patients undergoing Whipple procedure for clinically suspected carcinoma: a single-institution experience. *Am J Surg* 2006; **191**: 437–41. doi: https://doi.org/10.1016/j.amjsurg.2005.10.051
42. Berland LL, Silverman SG, Gore RM, Mayo-Smith WW, Megibow AJ, Yee J, et al. Managing incidental findings on abdominal CT: white paper of the ACR incidental findings committee. *J Am Coll Radiol* 2010; **7**: 754–73. doi: https://doi.org/10.1016/j.jacr.2010.06.013
43. Li C, Lin X, Hui C, Lam KM, Zhang S. Computer-aided diagnosis for distinguishing pancreatic mucinous cystic neoplasms from serous oligocystic adenomas in spectral CT images. *Technol Cancer Res Treat* 2016; **15**: 44–54. doi: https://doi.org/10.1177/1533034614563013
44. Kartalis N, Mucelli RM, Sundin A. Recent developments in imaging of pancreatic neuroendocrine tumors. *Ann Gastroenterol* 2015; **28**: 193–202.
45. Tamm EP, Bhosale P, Lee JH, Rohren EM. State-of-the-art Imaging of Pancreatic Neuroendocrine Tumors. *Surg Oncol Clin N Am* 2016; **25**: 375–400. doi: https://doi.org/10.1016/j.soc.2015.11.007
46. Lin XZ, Wu ZY, Tao R, Guo Y, Li JY, Zhang J, et al. Dual energy spectral CT imaging of insulinoma-Value in preoperative diagnosis compared with conventional multi-detector CT. *Eur J Radiol* 2012; **81**: 2487–94. doi: https://doi.org/10.1016/j.ejrad.2011.10.028
47. Yuan Y, Huang ZX, Li ZL, Bin S, Deng LP. Dual-source dual-energy computed tomography imaging of acute necrotizing pancreatitis–Preliminary study. *Sichuan Da Xue Xue Bao Yi Xue Ban* 2011; **42**: 691–4.
48. Yuan Y, Huang ZX, Li ZL, Song B, Deng LP. The value of dual-source dual-energy CT with iodine overlay in the diagnosis of acute necrotizing pancreatitis. *Sichuan Da Xue Xue Bao Yi Xue Ban* 2012; **43**: 597–600.
49. Yang CB, Zhang S, Jia YJ, Duan HF, Ma GM, Zhang XR, et al. Clinical application of dual-energy spectral computed tomography in detecting cholesterol gallstones from surrounding bile. *Acad Radiol* 2017; **24**: 478–82. doi: https://doi.org/10.1016/j.acra.2016.10.006

50. Uyeda JW, Sodickson AD. *Noncalcified Gallstones: Making the Invisible Visible with Dual Energy CT*. Chicago, IL: RSNA; 2015.
51. Oldan J, He M, Wu T, Silva AC, Li J, Mitchell JR, et al. Pilot study: Evaluation of dual-energy computed tomography measurement strategies for positron emission tomography correlation in pancreatic adenocarcinoma. *J Digit Imaging* 2014; **27**: 824–32. doi: https://doi.org/10.1007/s10278-014-9707-y
52. Bali MA, Metens T, Denolin V, Delhaye M, Demetter P, Closset J, et al. Tumoral and nontumoral pancreas: correlation between quantitative dynamic contrast-enhanced MR imaging and histopathologic parameters. *Radiology* 2011; **261**: 456–66. doi: https://doi.org/10.1148/radiol.11103515